



## Light-responsive bicyclic peptides†

Cite this: DOI: 10.1039/c7ob03178e

Mohammad R. Jafari,<sup>a</sup> Hongtao Yu,<sup>a,b</sup> Jessica M. Wickware,<sup>a</sup> Yu-Shan Lin <sup>a,b</sup> and Ratmir Derda  <sup>\*a</sup>

In this paper, we describe a method for the synthesis of light-responsive (LR) bicyclic macrocycles from linear peptides composed of 20 natural amino acids. Small molecules, peptide macrocycles, and protein conjugates that reversibly turn their function on and off in response to visible light enabled the fields of photopharmacology and optochemical genetics. Bioactive LR molecules could be produced by grafting azobenzene or other LR-structures onto molecules with known biological functions (e.g., alpha-helical peptides). It is also possible to discover such LR ligands *de novo* by selecting compounds with a desired function—such as binding to a target—from a library of LR-compounds or a genetically-encoded (GE) library of LR-macrocycles. The bicyclic topology of ligands offers added value such as improved binding and stability when compared to monocyclic peptides, but approaches for the design of bicyclic light-responsive architectures are limited. To address this need, we developed a tridentate C2-symmetric hydroxyl amine and di-chlorobenzene containing azobenzene (**HADCAz**) LR-linker with two orthogonally reactive functionalities (chlorobenzyl and hydroxylamine) to convert a linear unprotected peptide into a bicyclic peptide in a one-pot, two-step reaction. This linker reversibly isomerizes from the *trans* to *cis* form upon irradiation with blue light (365 nm). The resulting bicyclic peptide contains two loops of amino acids, one of which is constrained with an azobenzene moiety that can change the conformation in response to visible light. A scalable synthetic route to the **HADCAz** linker allowed us to demonstrate its application in multiple synthetic bicyclic peptides with loops that contain 2–5 amino acids.

Received 25th December 2017,  
Accepted 13th March 2018

DOI: 10.1039/c7ob03178e

rsc.li/obc

## Introduction

Photoswitchable ligands that reversibly change their affinity to a specific molecular target in response to light are powerful tools for the investigation of biological systems with spatial and temporal resolution. The emerging fields of photopharmacology<sup>1</sup> and optochemical genetics<sup>2</sup> are empowered by the discovery of novel light-responsive molecules that can be actuated from the “bioactive” to “inactive” state with visible light. The rational combination of photochromic compounds such as azobenzenes, spiropyrans and diarylethenes with known bioactive small molecules, peptides, and proteins has successfully yielded light-responsive ligands for tubulin,<sup>3</sup> NMDA receptors,<sup>4,5</sup> glucagon-like peptide-1 receptor (GLP-1R),<sup>6</sup> TRPV1,<sup>7</sup> ion channels,<sup>8–10</sup> specific DNA sequences,<sup>11,12</sup> Bcl-XL,<sup>13</sup>  $\beta$ -adaplin,<sup>14</sup> and histone deacetylases (HDACs)<sup>15,16</sup> (for an in-depth review see ref. 17). Light-responsive ligands have not been designed yet for many targets, and such a molecular

design would require significant efforts. The discovery of “static” bioactive ligands from combinatorial chemical libraries is a cornerstone of the modern pharmaceutical industry and chemical biology. It is thus attractive to repurpose the power of combinatorial and genetically-encoded screening to develop a versatile suite of discovery strategies for light-responsive bioactive molecules.

Peptides and their chemical derivatives constitute many of the biologically active compounds such as hormones, neurotransmitters, toxins and therapeutic agents. There are more than 60 FDA-approved peptide therapeutics on the market and more than 140 peptide candidates in clinical trials.<sup>18</sup> Many therapeutic leads have cyclic and bicyclic topology; 23 out of the 60 FDA-approved peptide drugs have a cyclic structure.<sup>19</sup> The advantages of bicyclic topology include high binding affinity,<sup>20,21</sup> increased stability to enzymatic hydrolysis,<sup>20,22</sup> and improved permeability through the cell membrane,<sup>23,24</sup> for cyclic peptides when compared to linear peptide precursors. The macrocyclization of a peptide through an intermolecular reaction with small molecule linkers or “linchpins” is now used as a common, versatile strategy for introducing light-responsiveness into the peptide.<sup>25</sup> For example, the chemical modification of  $\alpha$ -helical and  $\beta$ -hairpin<sup>26,27</sup> peptides with azobenzene is now used as a general, versatile solution for the conversion of bioactive peptides to LR-ligands. The use

<sup>a</sup>Department of Chemistry, University of Alberta, Edmonton, AB T6G2G2, Canada.  
E-mail: ratmir@ualberta.ca

<sup>b</sup>Department of Chemistry, Tufts University, Medford, Massachusetts 02155, USA

†Electronic supplementary information (ESI) available. See DOI: 10.1039/c7ob03178e

of peptides composed of unprotected natural amino acids and translationally-made polypeptide sequences in such modifications is attractive because the peptides of natural origin such as expressed proteins, phage-displayed peptide libraries, or mRNA-displayed libraries, are high-value “starting materials”. Million-to-billion scale genetically-encoded libraries of LR-ligands can be produced simply by grafting a light-responsive Azb-linchpin onto two thiol-reactive groups.<sup>28,29</sup> The groups of Heinis,<sup>28</sup> Ito<sup>30</sup> and Derda<sup>29</sup> have implemented such strategies to modify phage-displayed peptides,<sup>31</sup> phage-displayed libraries of peptides and mRNA-displayed libraries of peptides. These libraries were shown to be a productive source for the discovery of macrocycles that bind streptavidin with binding that can be either turned “on”<sup>28</sup> or “off”<sup>29</sup> by irradiation with light.

Bicyclic peptides are high-value molecular scaffolds for the discovery of potent ligands for diverse protein targets. To date, there is no general topological solution for the synthesis of light-responsive bicyclic peptides. To form  $n$  cycles in a peptide,  $n + 1$  points should be connected through a linchpin with  $n + 1$  reactive functionalities. For example, di- and tri-bromomethyl benzene (**DBMB** and **TBMB**, respectively, Fig. 1A) are classical static  $C_{2v}$  and  $C_{3v}$  symmetrical linchpins employed by Timmerman and coworkers to convert linear unprotected peptide chains with two or three cysteines into mono- and bicyclic peptides.<sup>32</sup> It is conceptually simple to upgrade static

bidentate  $C_{2v}$  symmetric linchpins to  $C_{2v}$  linchpins that contain LR-moieties, such as Azb, to form LR-cyclic peptide macrocycles. An example of such a linchpin is BSBCA (Fig. 1A).<sup>12,25</sup> Devising a LR-linchpin with three attachment points is not obvious, because all functionalities that undergo light-induced isomerization—such as azobenzenes, diarylethenes,<sup>33–35</sup> spiropyranes<sup>36,37</sup>—have lower  $C_{2v}$  symmetry. Wegner, Heinis and co-workers reported a synthesis of a putative  $C_{3v}$ -symmetric linchpin for the modification of peptides with three cysteines.<sup>38</sup> The authors, however, admitted that the use of two tandem Azb functionalities in a linchpin was not optimal because these moieties isomerize independently, yielding a poor light-switching performance. The use of a non- $C_{3v}$  symmetric linchpin with three identical reactive groups is impractical because its reaction with a peptide yields three or more constitutional isomers.

A viable topological solution for the synthesis of LR-bicycles uses a  $C_{2v}$  symmetric linchpin with 2 + 1 reactive groups that target 2 and 1 orthogonally-reactive functionalities in a peptide. Two types of LR-linchpins (LRLs) can be designed: (i) an LRL with two dynamic loops, both containing an Azb photo-switch and (ii) an LRL with one dynamic loop and one static loop. In this paper we implemented a  $C_{2v}$  linchpin that can form the latter bicycle with dynamic and static loops. We envision that one peptide ring can dynamically change its affinity to the receptor of interest, while the second ring can be reserved to introduce other static properties into the molecule, such as cell permeability (Fig. 1B and C).

## Results

In our design, the LR-linchpin should meet three criteria: (i) it should include functionalities that can selectively react with two orthogonally reactive handles present in or derived from natural amino acid side-chains. Herein, we focus on the thiol functionalities of cysteine and the glyoxal functionality produced from N-terminal serine by mild oxidation with sodium periodate.<sup>39</sup> (ii) The linker should have a half-life of thermal relaxation of more than 10 min after irradiation to provide sufficient time for potential biological studies, such as ligand–receptor interactions. (iii) The LRL should switch in response to visible light ( $\lambda_{\text{max}}$  of >360 nm), because most biological systems are sensitive to light with  $\lambda$  below 350 nm.<sup>40</sup>

We synthesized four different azobenzene cores (Fig. 2A, 1a–1d) which carried the suitable functionalities (–OH, –NH<sub>2</sub>, and Ar–OH) for further installation of cysteine and glyoxal-reactive groups. We did not observe any changes in the spectra after the irradiation of compounds 1a and 1b with 380 nm and 470 nm LEDs, respectively, which is most likely due to the fast thermal relaxation of azobenzene (Fig. S1A and B†). This is consistent with other published studies,<sup>40</sup> that found the single or double alkylation of one or both aromatic amines at either end of Azb to result in fast switching. Compound 1c exhibited the desired properties: its *trans* to *cis* isomerization was induced by irradiation with 380 nm light and the thermal

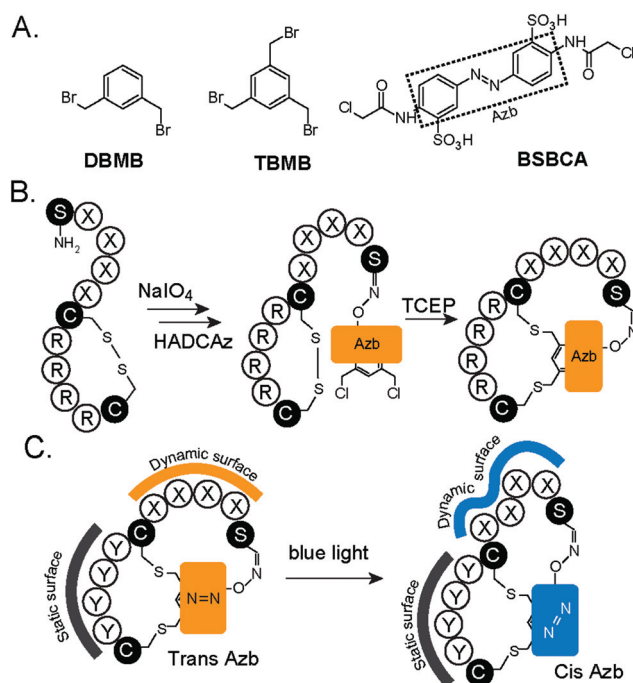


**Fig. 1** Strategy and linchpins for the synthesis of cyclic and bicyclic peptides with dynamic and/or static surfaces. (A) Thiol-reactive linchpins used for the generation of monocyclic (**DBMB**), bicyclic (**TBMB**), and monocyclic (**BSBCA**) LR-peptides. (B) Scheme of the synthesis of bicyclic LR-peptides from an unprotected linear peptide made of 20 natural amino acids. (C) A bicyclic LR-peptide may contain a static and a dynamic surface, each targeting a specific binding function.

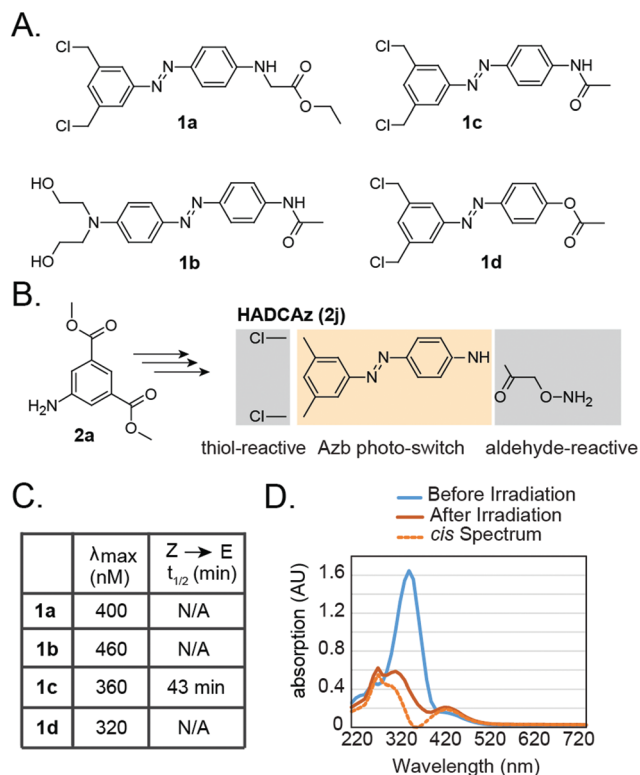
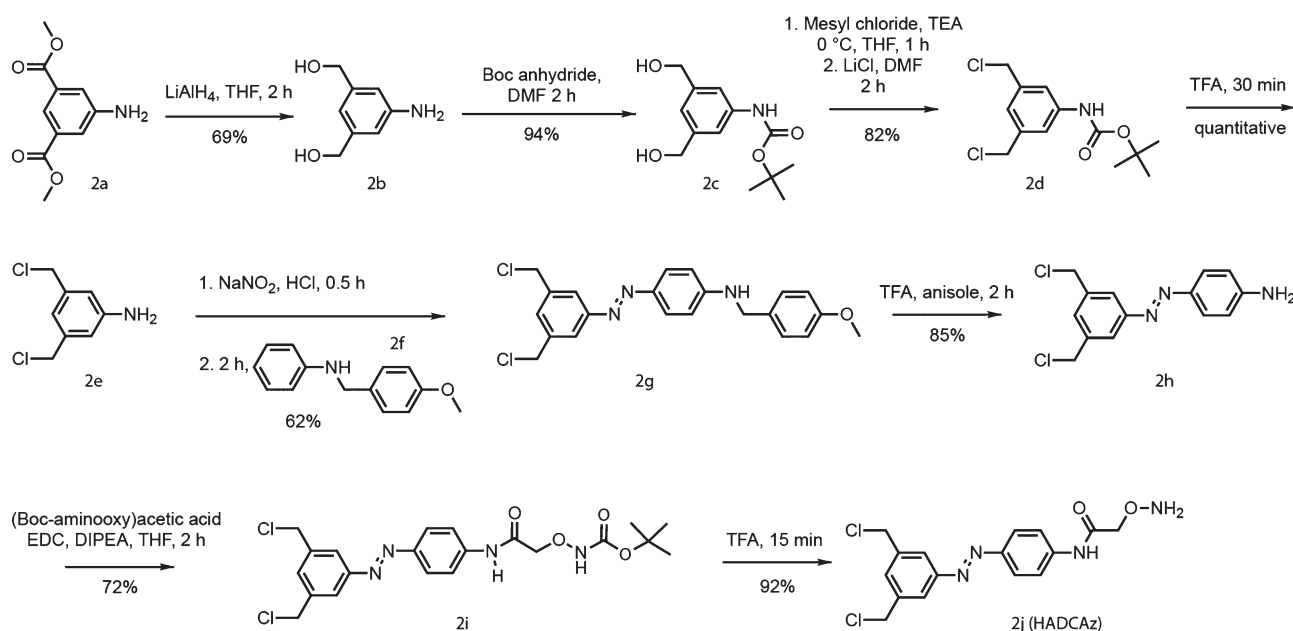


**Fig. 2** Synthesis of Azb cores and LR-linchpin **HADCAz**. (A) Potential Azb precursors to bicyclic macrocycles and their light-induced isomerization properties. (B) Minimalistic design of the light-responsive linker **HADCAz** for forming bicyclic macrocycles (see Scheme 1 for a complete synthetic route to **HADCAz**). (C) Light-induced isomerization properties of the precursor molecules shown in (A). (D) Absorption spectra of **HADCAz** before and after irradiation with 380 nm light.

relaxation of the *cis* form back to the *trans* form occurred with a half-life of 43 min (Fig. 2C).

The presence of an amide linkage in **1c** was crucial for an optimal light-response because core **1d**, in which the amide was replaced by an ester bond, showed the maximum absorption at 320 nm which is in the bio-incompatible UV region (Fig. S1D†). Based on the structure–activity relationship of the aforementioned azobenzenes, we believed that the arrangement of functional groups in azobenzene **1c** yielded near optimal photochemical properties (Fig. 2C and D). Installing the desired functional groups onto the Azb core **1c** (Fig. 2B) yielded hydroxyl amine, di-chlorobenzene containing azobenzene (**HADCAz**) in seven steps from dimethyl-5-(amino)isophthalate in 18.5% overall yield (Scheme 1). **HADCAz** exhibited maximum absorption at 350 nm, which is close to its parent Azb core **1c**. **HADCAz** was successfully switched to 71% *cis*-isomer in its photostationary state after irradiation with 365 nm light, and relaxed thermally to the *trans*-isomer with a half-life of ~60 min (Fig. 3).

To explore the utility of **HADCAz** for the bicyclization of peptides, we investigated the reaction of **HADCAz** with the peptide sequences  $\text{SX}_n\text{CRRRRC}$  where  $\text{X}_n$  was W, SW, KSW, or DKSW (Fig. 4A), which included the major reactive functionalities present in natural amino acids (amine, hydroxyl, carboxylic acid, and indole). The N-terminal serine can be converted to glyoxal, whereas cysteines flank a tetra-arginine sequence that has been used by Pei and co-workers to enhance the cell permeability of bicyclic peptides.<sup>41</sup> We found that forming the first cycle by the reaction of Cys with chlorobenzyls was not a suitable strategy, because the resulting sulfides are significantly more susceptible to periodate oxidation than the disulfides (Fig. 4C).<sup>42</sup> Adducts with +16 Da and +32 Da in the mass spectrum confirmed the oxidation of sulfides



**Scheme 1** Synthetic pathway for **HADCAz**.

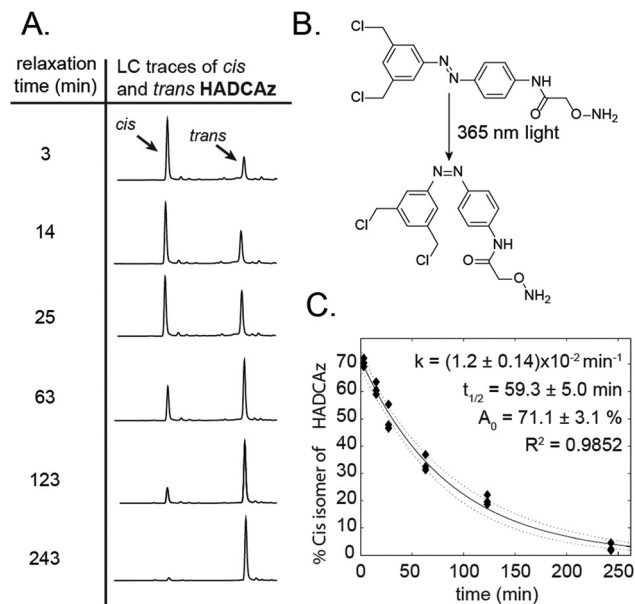


**Fig. 3** Thermal relaxation of HADCAz. (A) LCMS traces of the thermal relaxation of HADCAz after irradiation with 365 nm light. (B) Scheme of the isomerization of *trans*-HADCAz to the *cis* form. (C) Fitting the thermal relaxation data to the first order kinetics model determined the *cis*-ratio to be 71% in its photostationary state after irradiation, and the thermal relaxation half-life to be 59 min.

(Fig. S4†). In contrast, the oxidation of a disulfide peptide (Fig. 4A) with sodium periodate at pH 7.0 yielded a peptide glyoxal with an intact disulfide bond. Our attempt to perform

oxime ligation between the purified peptide glyoxal and HADCAz in water or water-organic mixtures such as 50% aqueous DMF (pH 4.5) was unsuccessful and yielded no apparent conversion (Fig. S3D–F†). The aniline catalyst (100 mM, pH 4.5)<sup>43</sup> accelerated these reactions but, unfortunately, it also gave rise to the nucleophilic substitution of the benzyl chlorides of HADCAz by aniline (Fig. 4D and Fig. S3G–H†). The most optimal oxime bond formation conditions involved adding the lyophilized peptide glyoxal to a DMF solution of HADCAz (1.2 eq.). The reaction was complete in 2 h at 55 °C (Fig. 4A) or after 24 h of incubation at room temperature (Fig. S3A–C†). Once the oxime bond was formed, the subsequent bicyclization of **7** was straightforward. Introducing three equivalents of TCEP into the reaction mixture resulted in the double intramolecular nucleophilic substitution of both chlorine atoms with the thiols yielding the quantitative “peak-to-peak conversion” of monocycle **7** to bicycle **8** (Fig. 4B). HRMS confirmed the identity of the bicycle.

We note that there exists an alternative cyclization pathway that starts with an alkylation of thiols in intermediate **6** by HADCAz (Fig. 4E). We observed that subsequent cyclization *via* the intramolecular formation of the oxime bond was not reproducible as it often yielded a significant amount of insoluble byproducts. It is tempting to suggest that the difference in the efficiency in bicyclization *via* **7**→**8** vs. **9**→**8** pathways originates from different geometric constraints of nucleophilic substitution and addition reactions. It is possible that the *exo*-tet cyclization of **7** to yield **8** is geometrically relaxed because it involves an acceptor on the freely-rotating benzylic bonds. In contrast, the formation of **8** from precursor **9** requires con-

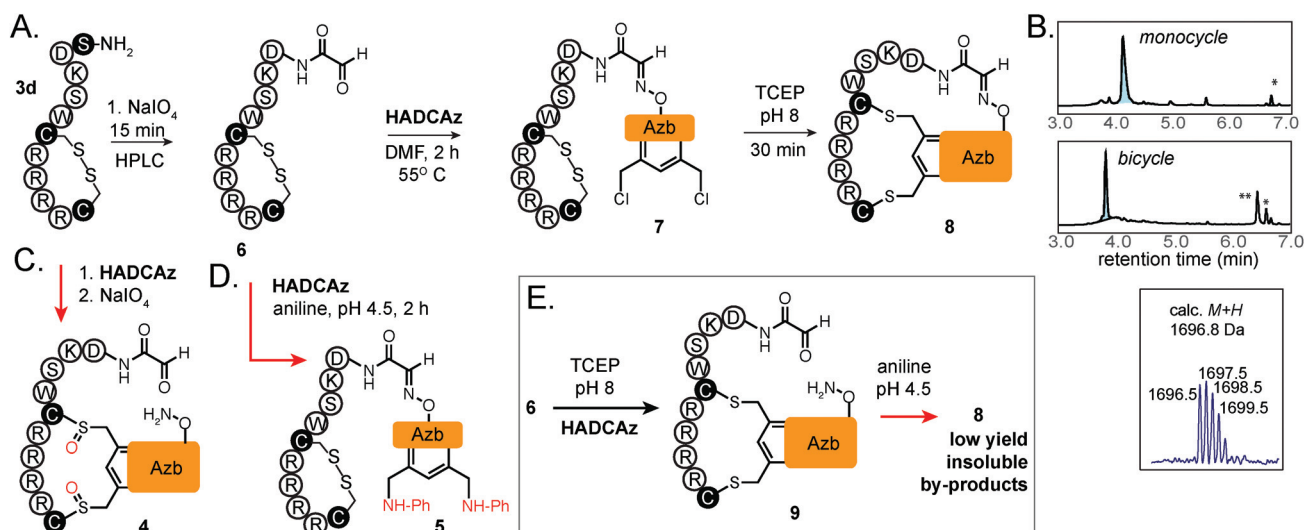


**Fig. 4** Synthetic pathways for the generation of LR-bicyclic peptides. (A) Successful route to bicyclization starts from the oxidative conversion of N-terminal serine to glyoxal followed by the reaction with HADCAz to form an oxime bond; subsequent reduction of the disulfide bond with TCEP triggers the intramolecular formation of two thioether bonds to close both cycles. (B) Conversion of monocycle **7** to bicycle **8** occurs as quantitative “peak-to-peak” conversion when monitored by HPLC. Mass-spectrometry confirmed the identity of the bicycle. (C–E) Plausible but unsuccessful routes to the same product. (C) Formation of the first cycle through thioether bonds is not a suitable first step because subsequent periodate oxidation results in the oxidation of the thioethers. (D) Oxime formation in the presence of aniline results in the undesired substitution of either one or both chlorines by aniline. (E) Although it is possible to convert intermediate **6** to monocyclic precursor **9**, its cyclization to the desired product **8** was inconsistent, and yielded a significant amount of uncharacterized insoluble byproducts (possibly oligomeric analogs of **8**).



**Table 1** Isolated yield, thermal relaxation half-life, and the ratio of the *cis*-isomer in the photostationary state after irradiation of peptides **3a–3d**

	Sequence	Isolated yield (%)	Relaxation half-time (min)	<i>cis</i> -Isomer in the photostationary state (%)
<b>3a</b>	SWCRRRRC	11	144.3 ± 18.7	86.2 ± 2.0
<b>3b</b>	SSWCRRRRC	74	243.1 ± 33.4	91.0 ± 1.9
<b>3c</b>	SKSWCRRRRC	63	117.2 ± 21.0	81.9 ± 1.5
<b>3d</b>	SDKSWCRRRRC	68	29.5 ± 1.3	74.9 ± 3.3

strained *endo*-trig cyclization with the acceptor orbital being part of an oxaloyl functionality that contains no rotating bonds (due to extended conjugation).

Optimized bicyclization conditions (Fig. 4A) occurred reproducibly for peptides with the structure of  $SX_nCR_4C$ , where  $n > 1$ . For  $X_n = SW, KSW$  or  $DSKW$ , the isolated yields were 74%, 63% and 68%, respectively (Table 1). HRMS and NMR spectroscopy confirmed the structures of all products (Fig. S2A–C†). The isolated yield for the peptide sequence SWCRRRRC ( $n = 1$ ) was lower (11%) and the reaction contained a mixture of unidentified byproducts (Fig. S2D†). The low yield of the reaction for this sequence highlights the lower limit of the bicyclization. The distance between the cysteine and glyoxal functionalities has to be at least two amino acids. To investigate the upper limit, we foresee studying the bicyclization with several peptide sequences  $SX_nCR_4C$  where  $X_n$  is 10–20 amino acids.

Bicyclic products **3a–3d** successfully switched to their *cis*-isomers after irradiation with 365 nm light, as indicated by a decrease in their absorption at 350 nm (Fig. S5†). We determined the ratio of the *cis*-isomer to *trans*-isomer for each peptide by LCMS in time intervals after irradiation (Fig. S6A†). Fitting the data to a first order kinetics model determined the relative amount of the *cis* isomer in the photostationary state (Fig. S6B†). Interestingly, we found that the ratio of the *cis*-isomer in the photostationary state for bicyclic peptides **3a–3c** is higher than that for **HADCAz** alone (Table 1). The thermal relaxation half-life for **3a**, **3b** and **3c** was 144, 243, and 117 min, respectively, which was higher than the half-life of **HADCAz** (59 min). The ratio of the *cis*-isomer in the photostationary state for **3d** was 75%, which was close to the *cis*-ratio of **HADCAz**; however, its thermal relaxation half-life dropped to 29 min. The higher *cis*-ratio and relaxation half-life of the products could be because of greater ring strain in **3a–3c**. We suspect that this modulation of photoswitching could also be sequence-specific, but the evaluation of different sequences extends beyond the scope of this paper.

To understand the changes in the conformation of peptides upon irradiation, we employed 100 ps molecular dynamics (MD) simulation in explicit TIP4P water for peptides **3a–3d** with the N=N bond constrained as the *cis*-state (“dark state”) or *trans*-state (“light state”) (details of the simulation are available in the ESI†). Although bicycles **3a–3d** do not exhibit a well-defined structure to be detected by NMR, MD simulations of bicycles **3a–3d** predict an ensemble of structures with Azb

in the *trans*-state and *cis*-state that shed some light on the potential changes in the conformation of the peptides and the azobenzene core in response to illumination. Fig. S14 and S15† contain selected structures and Derda\_PDB.zip has PDB of all structures. The most remarkable observation was that the 198/200 MD simulations of “dark” **3a** (ground state) converged on structures that contained the *cis*-configuration for the aromatic amide bond nearest to the azobenzene. In “light” **3a** structures, all amide bonds were of *trans*-configuration (Fig. 5). The same amide bond was of *cis*-configuration with a 73/200 conformation of simulated “dark” **3b** structures (Fig. S16†). “Dark” **3c** and **3d** contained *cis* amide bonds in only 4/200 conformations (Fig. S16†). UV spectroscopy corroborated that the N=N bond in the “dark” state **3a** is indeed *trans* (Fig. S5†). ROESY NMR spectroscopy confirmed that the aromatic amide bond is indeed uniquely *cis* in “dark” **3a** (Fig. 5C and S17†), whereas it is *trans* in “dark” **3b–3d** (Fig. S17 and page S81 of the ESI†). In 1D NMR spectroscopy, the proton of this amide bond exhibited a change in the chemical shift from 9.4 ppm in **3a** to 9.7 ppm in **3b**, **3c** and **3d** (see the ESI, page S77†). Combined evidence from the MD simulation and spectroscopy, thus, suggest that the smallest bicycle **3a** cannot simultaneously contain a *trans* N=N bond and all amide bonds in the *trans*-configuration. The aromatic amide bond, which has the lowest rotational barrier, has to adopt the *cis*-conformation in the “dark” *trans* (N=N) state. As **3a** is photoexcited to the *cis* (N=N) state, the backbone geometry is relaxed and the aromatic amide bond can adopt the *trans*-conformation. The relaxation of the amide bond predicted by MD simulation to the *trans* state upon light irradiation of **3a** could be further confirmed in the future by NMR spectroscopy of the irradiated bicycle **3a**.

## Discussion

In conclusion, we developed a  $C_{2v}$  symmetric, tridentate LR-linchpin that can react with peptides of the structure  $SX_nCX_mC$  to form LR-bicyclic macrocycles. The reaction occurs site-specifically on unprotected peptides consisting of only natural amino acids and cyclization results in satisfactory yields for peptides that contain a medium sized ring ( $n > 1$ ). The dynamic loop of the bicyclic products ( $SX_nC$ ) contained an azobenzene moiety which was successfully switched to its *cis*-isomer in response to 365 nm light for  $n = 1–4$ . The number of amino acids in the loop modulates the switching properties of the product. The static ring of the molecule harbors a tetra-arginine sequence which has been shown to increase the permeability of bicyclic peptides into mammalian cells. We were not able to perform oxime ligation under aqueous conditions, and the current **HADCAz** bicyclization reaction is incompatible with potentially attractive applications such as the modification of proteins or phage-displayed peptides.<sup>29,31</sup> Further investigation will be required to identify suitable aqueous reaction conditions, or to integrate another existing N-terminal ligation method into our reaction.<sup>44</sup>

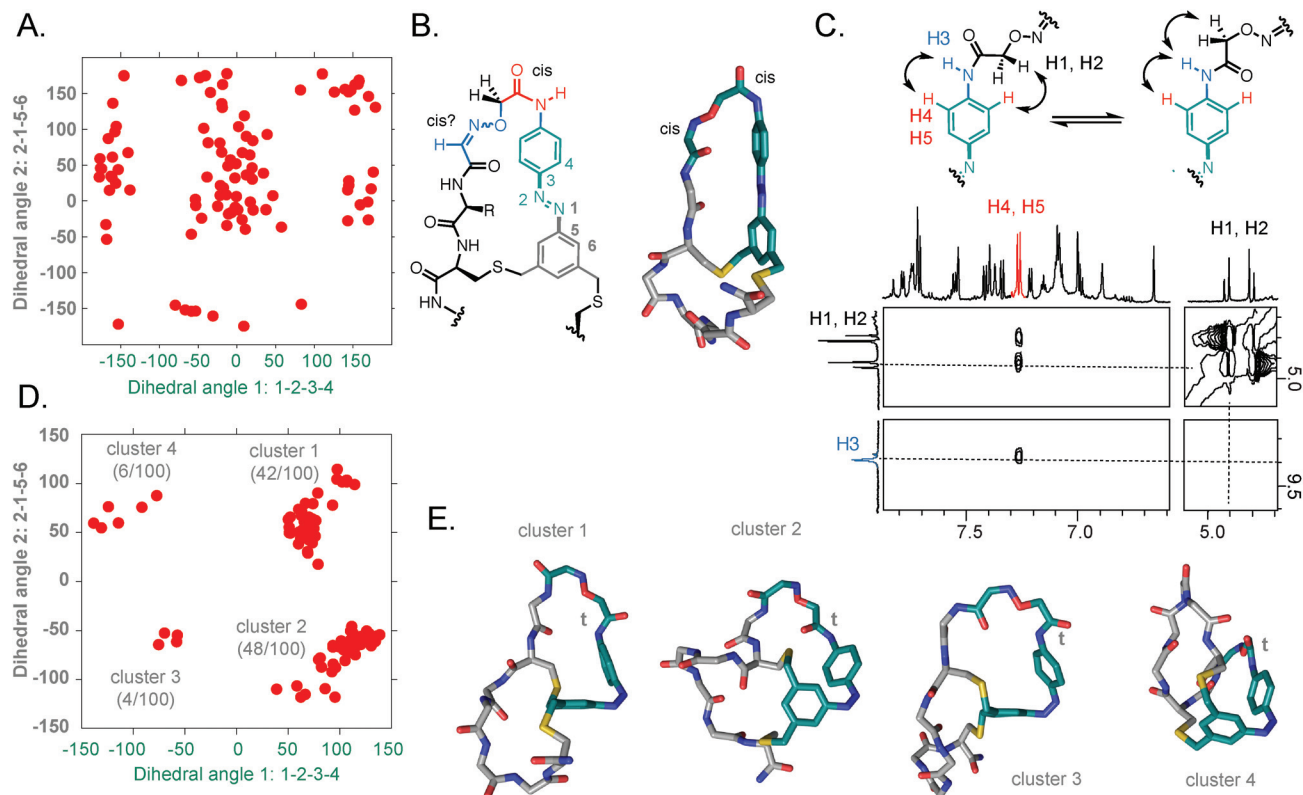


**Fig. 5** Molecular dynamics (MD) analysis of the photoisomerization of the smallest bicycle **3a**. (A) Conformational preferences of dihedral angles adjacent to the core N=N functionality in the HADCAz crosslinker in azo-*trans*-**3a** ("dark **3a**") (B) after 100 MD simulations in TIP4P water. The structures of both HADCAz and the peptide backbone diverged in 100 simulations (see Fig. S14,† and PDB files in Derda\_PDB.zip in the ESI†). Interestingly, every structure enforced the *cis*-configuration for the aromatic amide adjacent to HADCAz. The same MD simulation predicted the *trans*-amide bond in dark **3b**, **3c** and **3d** (Fig. S15 and S16†). (C) ROESY NMR spectroscopy confirmed the *cis*-configuration of the amide bond in dark **3a**: (i) we observed NOE interactions between (H1,H2) and (H4,H5), which is possible only in the *cis*-amide configuration; (ii) we observed no (H1,H2)–(H3) interactions present in **3b**, **3c** and **3d** that contain a *trans*-amide bond (Fig. S16, S17 and NOE summary on page S81†). (D) MD simulation of azo-*cis*-**3a** ("light **3a**") simulations in TIP4P water converged on well-defined clusters that lock azobenzene in two possible configurations. (E) Representative structures of *cis*-**3a** predicted by MD analysis (see Movie S1† for all structures). Every structure has a *trans*-configuration for the aromatic amide bond.

The requirement for the *cis* amide bond geometry in the ground state of **3a** detected by MD simulation and NMR spectroscopy explains the dramatic decrease in the yield of the bicyclization reaction (11%, Table 1 and Fig. S13†). The relaxation of the geometric constraints in the photoexcited state suggests that the yield of this bicyclization with the HADCAz linker in small peptides could be increased if the reaction is performed under light irradiation, forcing the HADCAz linker to adopt the *cis*-conformation. The platform we described in this paper could be employed in the future for the development of ligands that dynamically regulate cell functions *via* binding to intracellular signalling components. Such bicyclic LR-inhibitors will expand the growing toolbox of optochemical genetics<sup>2</sup> and photo-pharmacology,<sup>1</sup> and permit the investigation of cell signaling pathways that are not currently possible to study using conventional tools.

## Conflicts of interest

The corresponding author of this publication serves as the founder and CEO of 48Hour Discovery Inc.

## Acknowledgements

This work was supported by research grants from the National Science and Engineering Research Council of Canada (NSERC, #492943), NSERC Accelerator Supplement, and the Alberta Glycomics Centre. Infrastructure support was provided by the Canadian Foundation for Innovation (CFI) New Leaders Opportunity. We thank Mark Miskolzie and Ryan McKay for assistance in NMR spectra acquisition and interpretation and Dr. Nicholas J. Bennett for assistance with the alignment and visualization of PDB structures. JMW was supported by an Alberta Innovates—Summer Studentship.

## References

- W. A. Velema, W. Szymanski and B. L. Feringa, *J. Am. Chem. Soc.*, 2014, **136**, 2178.
- T. Fehrentz, M. Schonberger and D. Trauner, *Angew. Chem., Int. Ed.*, 2011, **50**, 12156.
- M. Borowiak, W. Nahaboo, M. Reynders, K. Nekolla, P. Jalinet, J. Hasserodt, M. Rehberg, M. Delattre, S. Zahler,

- A. Vollmar, D. Trauner and O. Thorn-Seshold, *Cell*, 2015, **162**, 403.
- 4 S. Berlin, S. Szobota, A. Reiner, E. C. Carroll, M. A. Kienzler, A. Guyon, T. Xiao, D. Trauner and E. Y. Isacoff, *eLife*, 2016, **5**, DOI: 10.7554/eLife.12040.
  - 5 L. Laprell, E. Repak, V. Franckevicius, F. Hartrampf, J. Terhag, M. Hollmann, M. Sumser, N. Rebola, D. A. DiGregorio and D. Trauner, *Nat. Commun.*, 2015, **6**, 8076.
  - 6 J. Broichhagen, T. Podewin, H. Meyer-Berg, Y. von Ohlen, N. R. Johnston, B. J. Jones, S. R. Bloom, G. A. Rutter, A. Hoffmann-Roder, D. J. Hodson and D. Trauner, *Angew. Chem., Int. Ed.*, 2015, **54**, 15565.
  - 7 J. A. Frank, M. Moroni, R. Moshourab, M. Sumser, G. R. Lewin and D. Trauner, *Nat. Commun.*, 2015, **6**, 7118.
  - 8 M. Volgraf, P. Gorostiza, S. Szobota, M. R. Helix, E. Y. Isacoff and D. Trauner, *J. Am. Chem. Soc.*, 2007, **129**, 260.
  - 9 M. Volgraf, P. Gorostiza, R. Numano, R. H. Kramer, E. Y. Isacoff and D. Trauner, *Nat. Chem. Biol.*, 2006, **2**, 47.
  - 10 D. L. Fortin, M. R. Banghart, T. W. Dunn, K. Borges, D. A. Wagenaar, Q. Gaudry, M. H. Karakossian, T. S. Otis, W. B. Kristan, D. Trauner and R. H. Kramer, *Nat. Methods*, 2008, **5**, 331.
  - 11 A. M. Caamano, M. E. Vazquez, J. Martinez-Costas, L. Castedo and J. L. Mascarenas, *Angew. Chem., Int. Ed.*, 2000, **39**, 3104.
  - 12 L. Guerrero, O. S. Smart, G. A. Woolley and R. K. Allemann, *J. Am. Chem. Soc.*, 2005, **127**, 15624.
  - 13 S. Kneissl, E. J. Loveridge, C. Williams, M. P. Crump and R. K. Allemann, *ChemBioChem*, 2008, **9**, 3046.
  - 14 A. Martin-Quiros, L. Nevola, K. Eckelt, S. Madurga, P. Gorostiza and E. Giralt, *Chem. Biol.*, 2015, **22**, 31.
  - 15 S. A. Reis, B. Ghosh, J. A. Hendricks, D. M. Szantai-Kis, L. Tork, K. N. Ross, J. Lamb, W. Read-Button, B. X. Zheng, H. T. Wang, C. Salthouse, S. J. Haggarty and R. Mazitschek, *Nat. Chem. Biol.*, 2016, **12**, 317.
  - 16 W. Szymanski, M. E. Ourailidou, W. A. Velema, F. J. Dekker and B. L. Feringa, *Chem. – Eur. J.*, 2015, **21**, 16517.
  - 17 R. J. Mart and R. K. Allemann, *Chem. Commun.*, 2016, **52**, 12262.
  - 18 K. Fosgerau and T. Hoffmann, *Drug Discovery Today*, 2015, **20**, 122.
  - 19 P. Vlieghe, V. Lisowski, J. Martinez and M. Khrestchatsky, *Drug Discovery Today*, 2010, **15**, 40.
  - 20 C. Heinis, T. Rutherford, S. Freund and G. Winter, *Nat. Chem. Biol.*, 2009, **5**, 502.
  - 21 J. Löfblom, J. Feldwisch, V. Tolmachev, J. Carlsson, S. Ståhl and F. Y. Frejd, *FEBS Lett.*, 2010, **584**, 2670.
  - 22 Á. Roxin and G. Zheng, *Future Med. Chem.*, 2012, **4**, 1601.
  - 23 E. A. Villar, D. Beglov, S. Chennamadhavuni, J. A. Porco Jr., D. Kozakov, S. Vajda and A. Whitty, *Nat. Chem. Biol.*, 2014, **10**, 723.
  - 24 Q. Chu, R. E. Moellering, G. J. Hilinski, Y.-W. Kim, T. N. Grossmann, J. T. H. Yeh and G. L. Verdine, *MedChemComm*, 2015, **6**, 111.
  - 25 D. C. Burns, F. Zhang and G. A. Woolley, *Nat. Protoc.*, 2007, **2**, 251.
  - 26 A. Aemissegger, V. Krautler, W. F. van Gunsteren and D. Hilvert, *J. Am. Chem. Soc.*, 2005, **127**, 2929.
  - 27 S. L. Dong, M. Loweneck, T. E. Schrader, W. J. Schreier, W. Zinth, L. Moroder and C. Renner, *Chem. – Eur. J.*, 2006, **12**, 1114.
  - 28 S. Bellotto, S. Chen, I. Rentero Rebollo, H. A. Wegner and C. Heinis, *J. Am. Chem. Soc.*, 2014, **136**, 5880.
  - 29 M. R. Jafari, L. Deng, P. I. Kitov, S. Ng, W. L. Matochko, K. F. Tjhung, A. Zeberoff, A. Elias, J. S. Klassen and R. Derda, *ACS Chem. Biol.*, 2013, **9**, 443.
  - 30 M. Z. Liu, S. Tada, M. Ito, H. Abe and Y. Ito, *Chem. Commun.*, 2012, **48**, 11871.
  - 31 M. R. Jafari, J. Lakusta, R. J. Lundgren and R. Derda, *Bioconjugate Chem.*, 2016, **27**, 509.
  - 32 P. Timmerman, J. Beld, W. C. Puijk and R. H. Meloen, *ChemBioChem*, 2005, **6**, 821.
  - 33 T. Fukaminato, T. Hirose, T. Doi, M. Hazama, K. Matsuda and M. Irie, *J. Am. Chem. Soc.*, 2014, **136**, 17145.
  - 34 O. Babii, S. Afonin, M. Berditsch, S. Reisser, P. K. Mykhailiuk, V. S. Kubyshev, T. Steinbrecher, A. S. Ulrich and I. V. Komarov, *Angew. Chem., Int. Ed.*, 2014, **53**, 3392.
  - 35 C. C. Warford, V. Lemieux and N. R. Branda, in *Molecular Switches*, 2nd edn, 2011, vol. 1, p. 1.
  - 36 L. Chen, J. Wu, C. Schmuck and H. Tian, *Chem. Commun.*, 2014, **50**, 6443.
  - 37 R. Klajn, *Chem. Soc. Rev.*, 2014, **43**, 148.
  - 38 S. Bellotto, R. Reuter, C. Heinis and H. A. Wegner, *J. Org. Chem.*, 2011, **76**, 9826.
  - 39 K. F. Geoghegan and J. G. Stroh, *Bioconjugate Chem.*, 1992, **3**, 138.
  - 40 A. A. Beharry and G. A. Woolley, *Chem. Soc. Rev.*, 2011, **40**, 4422.
  - 41 W. Lian, B. Jiang, Z. Qian and D. Pei, *J. Am. Chem. Soc.*, 2014, **136**, 9830.
  - 42 B. J. Evans, J. T. Doi and W. K. Musker, *J. Org. Chem.*, 1990, **55**, 2580.
  - 43 A. Dirksen, T. M. Hackeng and P. E. Dawson, *Angew. Chem., Int. Ed.*, 2006, **45**, 7581.
  - 44 C. B. Rosen and M. B. Francis, *Nat. Chem. Biol.*, 2017, **13**, 697.